Journal of Physics: Condensed Matter

PAPER

Optical and transport properties correlation driven by amorphous/crystalline disorder in InP nanowires

To cite this article: H Kamimura *et al* 2016 *J. Phys.: Condens. Matter* **28** 475303

View the article online for updates and enhancements.

Related content

- Optoelectronic characteristics of single InP nanowire grown from solid source
  H Kamimura, C J Dalmaschio, S C Carrocine et al.
- Photocurrent enhancement and magnetoresistance in indium phosphide single nanowire by zinc doping
  Fernando Maia de Oliveira, Ivani Meneses Costa, Edson Rafael Cardozo de Oliveira et al.
- Defect induced structural inhomogeneity, ultraviolet light emission and near-band-edge photoluminescence broadening in degenerate In2O3 nanowires
  Souvik Mukherjee, Ketaki Sarkar, Gary P Wiederrecht et al.

Recent citations

- Photocurrent enhancement and magnetoresistance in indium phosphide single nanowire by zinc doping
  Fernando Maia de Oliveira *et al*

IOP | ebooks™

Bringing you innovative digital publishing with leading voices to create your essential collection of books in STEM research.

Start exploring the collection - download the first chapter of every title for free.

This content was downloaded from IP address 200.136.226.160 on 06/05/2019 at 14:45

IOP Publishing Journal of Physics: Condensed Matter
J. Phys.: Condens. Matter **28** (2016) 475303 (7pp) doi:10.1088/0953-8984/28/47/475303

Optical and transport properties correlation driven by amorphous/crystalline disorder in InP nanowires

H Kamimura[1], **R C Gouveia**[2], **S C Carrocine**[1], **L D Souza**[3], **A D Rodrigues**[1], **M D Teodoro**[1], **G E Marques**[1], **E R Leite**[4] **and A J Chiquito**[1]

[1] Departamento de Física, Universidade Federal de São Carlos, CEP 13565-905, CP 676, São Carlos, São Paulo, Brazil
[2] Instituto Federal de Educação, Ciência e Tecnologia de São Paulo, CEP 14169-263, Sertãozinho, São Paulo, Brazil
[3] Departamento de Matemática, Universidade Estadual do Centro-Oeste, CEP 84500-000, Irati—Paraná, Brazil
[4] Departamento de Química, Universidade Federal de São Carlos, CEP 13565-905, CP 676, São Carlos, São Paulo, Brazil

E-mail: hanay@df.ufscar.br

Received 4 June 2016, revised 5 September 2016
Accepted for publication 8 September 2016
Published 23 September 2016

Abstract

Indium phosphide nanowires with a single crystalline zinc-blend core and polycrystalline/amorphous shell were grown from a reliable route without the use of hazardous precursors. The nanowires are composed by a crystalline core covered by a polycrystalline shell, presenting typical lengths larger than 10 μm and diameters of 80–90 nm. Raman spectra taken from as-grown nanowires exhibited asymmetric line shapes with broadening towards higher wave numbers which can be attributed to phonon localization effects. It was found that optical phonons in the nanowires are localized in regions with average size of 3 nm, which seems to have the same order of magnitude of grain sizes in the polycrystalline shell. Regardless of the fact that the nanowires exhibit a crystalline core, any considerable degree of disorder can lead to a localized behaviour of carriers. In consequence, the variable range hopping was observed as the main transport instead of the usual thermal excitation mechanisms. Furthermore the hopping length was ten times smaller than nanowire cross-sections, confirming that the nanostructures do behave as a 3D system. Accordingly, the V-shape observed in PL spectra clearly demonstrates a very strong influence of the potential fluctuations on the exciton optical recombination. Such fluctuations can still be observed at low temperature regime, confirming that the amorphous/polycrystalline shell of the nanowires affects the exciton recombination in every laser power regime tested.

Keywords: InP nanowires, VLS growth, eletronic disorder

(Some figures may appear in colour only in the online journal)

1. Introduction

Semiconductor nanowires have attracted much attention in the last decade due to their potential for a vast range of applications including electronic, photonic, biological, energetic and magnetic devices [1]. Regarding the large surface-to-volume ratio, active regions of such devices are enlarged and some physical properties are also enhanced. Consequently the efficiency of a variety of devices built from these nanostructures is also increased, such as light, gas or chemical sensors.

Among the nanomaterials being studied, the indium phosphide (InP) is considered an attractive alternative since it is one of the III–V group semiconductors whose growth process involves less toxic compounds [2], and presents interesting

 © 2016 IOP Publishing Ltd Printed in the UK

optoelectronic characteristics: direct bandgap in the near-infrared spectral region between silicon and gallium arsenide gaps, allowing the fabrication of solar cells [3–5], photodetectors [6], lasers [7], and light-emitting diodes [8]. Being a material with low surface recombination velocity, InP optical properties are subject of intense investigation in the literature searching for enhanced optoelectronic device applications [4, 9, 10]. Also, InP is useful for electronic device fabrication showing good performance as field-effect devices [11, 12]. Furthermore, InP nanowires are being used in theoretical and experimental approaches for deep investigations on electron confinement in low dimensional structures [13–17]. Recently, theoretical findings also elucidate changes in absorption and radiative lifetimes of these nanoestructures [18, 19].

Reliable crystalline InP nanowires can be obtained from several growth methods [10, 20–22], and the enhanced control of these processes already demonstrated that new promising structures can also be fabricated, such as polytypic nanowires exhibiting alternating zinc-blend and wurtzite phases [9], core-shell [5], and twinned superlattice structures [23].

As a matter of fact, these promising optical and electrical properties make InP nanowires suitable for many applications. However the characteristic large surface-to-volume ratio observed in nanostructures also leads to an enhanced sensitivity to the presence of disorder. Disorder is one of the inherent features of self-assembled structures which affects the expected behaviour of devices. Usually, the disorder leads to localized behaviour of carriers transport and to a transition from a simple excitation semiconducting mechanism to another one, such as the variable range hopping (VRH) mechanism. This mechanism arises when a sufficient amount of disorder states causes the random component of the crystalline potential to be large enough to localize the electron wave functions near the band edges [24–26].

The purpose of this work is an investigation of the optoelectronic properties of indium phosphide nanowires displaying a single crystalline zinc-blend core and polycrystalline/amorphous shell grown from a reliable route of synthesis without the use of hazardous precursors. The paper is structured in the following way: firstly, synthesis and structural characterization of the nanowires are reported. The data were obtained from scanning electron microscopy, transmission electron microscopy and Raman spectroscopy; secondly, the device fabrication is described aiming the determination of the transport mechanism and for this task, temperature dependent resistance measurements were carried out; finally, optical properties of as-grown nanowires were studied by photoluminescence experiments, confirming the results provided by the other techniques and indicating the influence of the polycrystalline shell on the nanowires optical properties.

2. Experimental details

InP nanowires were grown by the well known vapour–liquid–solid (VLS) mechanism [27] on quartz substrates in a tube furnace using InP powder as precursor material and a mixture of He/H_2 as the carrier gas. In this method, gold seeds in the liquid-phase are the catalysts of the growth process, acting as a preferential site for the adsorption of vapour-phase and determining nanowire dimensions.

For Au catalyst fabrication, a 2 nm thick gold layer was evaporated onto quartz substrates and annealed at 600 °C, at pressure of 10^{-5} mbar. After 15 min the furnace temperature was lowered to 450 °C and the He/H_2 flux was adjusted to 20 sccm. Then, the InP powder was vaporized by an external heater, while the substrates were kept at the growth temperature by the furnace. When the growth process was completed, the precursor heater was turned off but the gas flux was maintained until the temperature decreased to 100 °C in order to avoid oxidation [28].

Raman scattering spectra were carried out using a standard micro Raman setup. The scattered light was dispersed by a triple grating monochromator and recorded by a CCD camera cooled by liquid nitrogen. The 514.5 nm line of an Ar^+ laser was used as excitation. The studied substrate presented a high nanowire density: in this random distribution some nanowires were suspended by other ones, resulting in a poor thermal contact between the nanostructures and the substrate. Therefore, any excess of energy supplied by the excitation source could heat the nanowires. In order to avoid such heating, the laser power was kept lower than 1 mW during the experiment. The adopted experimental configuration corresponds to a spectral resolution of 1.5 cm^{-1}.

In order to study the mechanism of electric conduction, resistance measurements were carried out varying the temperature from 100 to 400 K in a closed cycle helium cryostat at pressures lower than 10^{-6} mbar. The devices were built by direct evaporation of patterned metallic electrodes on the as-grown samples using a shadow mask in such a way that the electric current between the electrodes is transmitted only by nanowire junctions.

In order to further investigate effects of localized states on the electronic response, optical properties were investigated using photoluminescence (PL) technique in a wide temperature range (from 7 K to 300 K). A 660 nm diode laser was used for excitation and the luminescence was dispersed by a 75 cm spectrometer and detected by a Silicon CCD. The measurements were performed for 8 μW and 50 mW laser powers focused in a spot of 25 μm of diameter.

3. Results and discussion

3.1. Synthesis and structural characterization of the nanowires

Scanning electron microscopy (SEM) images, such as those shown in figures 1(a) and (b), allowed the formation of a thick and uniform layer ($\sim$20 μm) of nanowires covering the quartz substrates to be observed. These nanostructures presented lengths larger than 10 μm. The diameter distribution was statistically analysed, as shown in figure 1(c), providing typical nanowire diameters in the range 80–90 nm. Figure 1(d) depicts a high resolution transmission electron microscopy (HRTEM) image of a representative InP nanowire whose analyses were made in previous work [28]. Here it illustrates the crystalline

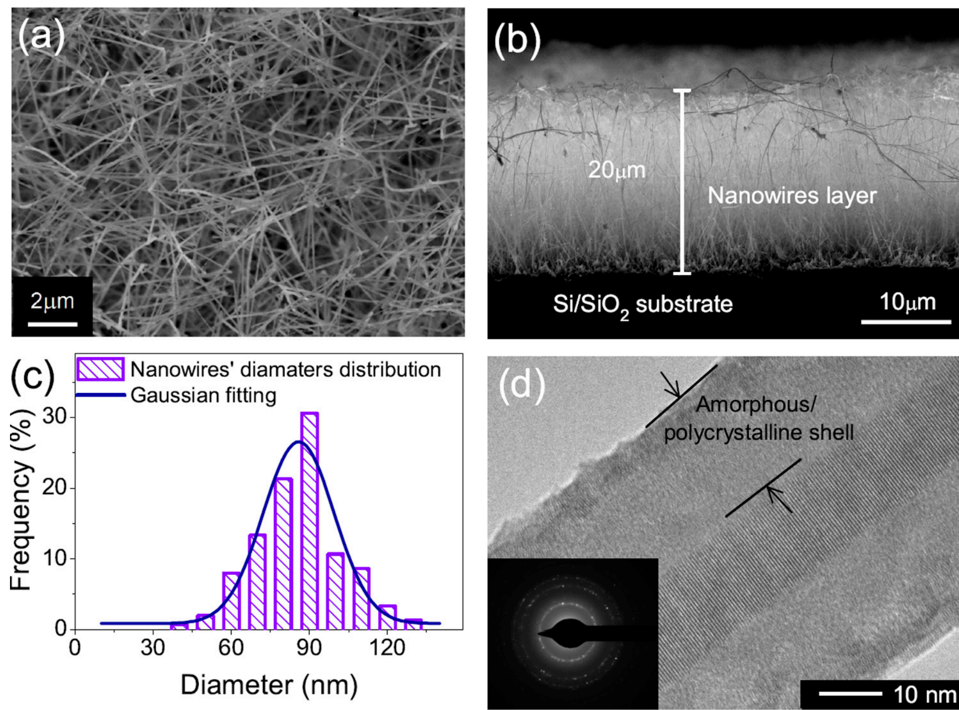

Figure 1. SEM image of as-grown samples from (a) up view and (b) side view, demonstrating the high density of nanowires forming a layer of 20 μm thickness over the Si/SiO_2 substrate. (c) The corresponding diameter distribution of the nanowires centred between 80 and 90 nm. (d) HRTEM image of a single nanowire, showing the InP crystalline core with an amorphous/polycrystalline layer composed by the same material and the corresponding typical polycrystalline SAED pattern (inset).

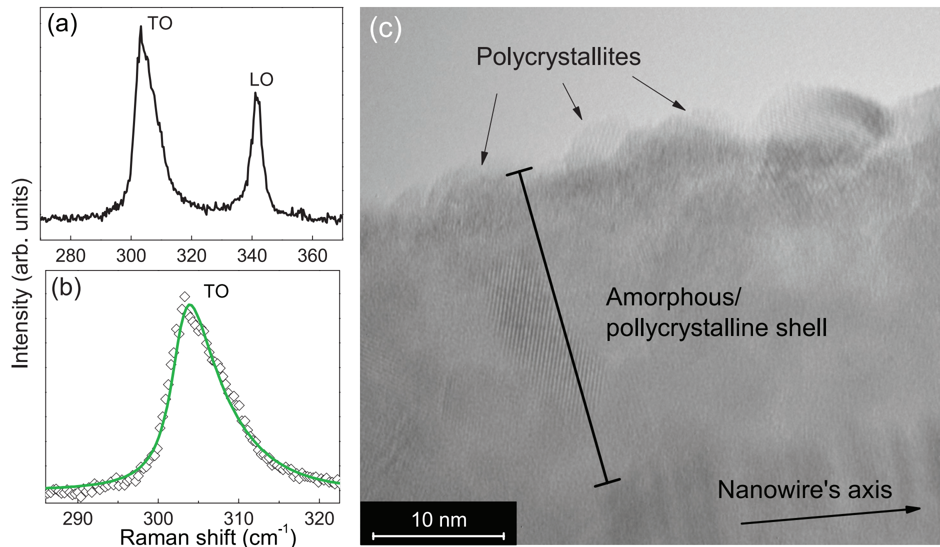

Figure 2. (a) Raman spectra of InP nanowires. (b) Experimental (diamonds) TO phonon and theoretical (green line) Raman spectrum, calculated using equation (1). (c) HRTEM image showing polycrystallites present in the nanowire shell.

core covered by an amorphous/polycrystalline layer, which is originated from the self-organized growth mechanism. The typical polycrystalline SAED pattern corresponding to the shell is shown in the inset.

Figure 2(a) presents the Raman spectrum of the InP nanowire where the peaks centered at 303 and 342 cm^{-1} correspond to the transversal optical (TO) and the longitudinal optical (LO) phonons of InP zinc-blende structure, respectively. The TO peak clearly presents an asymmetric line shape with broadening towards higher wave numbers. The presence of TO peaks with asymmetric shapes in the Raman spectrum measured in InP nanostructures is attributed to the activation of TO-phonons with momentum higher than zero (Γ-point) [29]. The confinement of phonons inside small crystalline portions leads to a relaxation of the $q = 0$ selection rule. Since the TO-phonons of InP present a positive dispersion relation, the relaxation of the selection rule allows phonons with higher wave numbers to participate in the Raman scattering, resulting in a peak with upward asymmetric shape. The consequent Raman intensity can be calculated by [30]

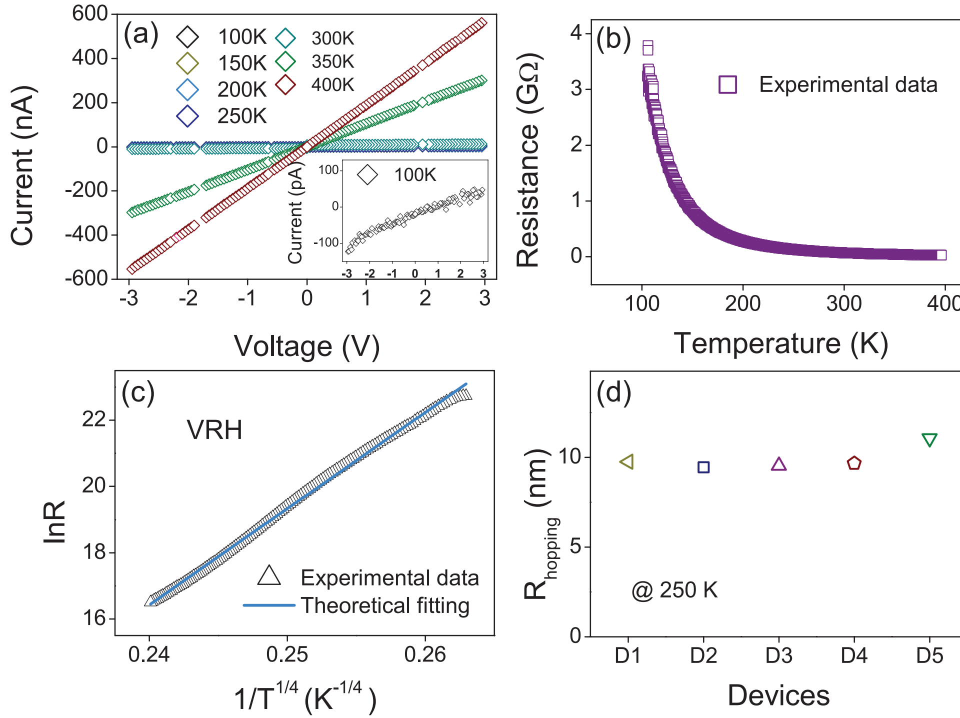

Figure 3. (a) Typical I–V ohmic characteristic of the devices with Ti contacts. (b) Temperature dependent resistance measurement, demonstrating a semiconductor behaviour. (c) Theoretical fitting of the resistance accordingly to the VRH model for temperatures ranging from around 100 to 250 K. (d) $R_{hopping}$ values at 250 K for the measured devices ($\Delta R = \pm 0.05$ nm).

$$I(\omega) \propto \int \exp\left(-\frac{q^2L_c^2}{4}\right)\frac{\mathrm{d}^3q}{[\omega-\omega(q)]^2+\left(\frac{\Gamma}{2}\right)^2}, \quad (1)$$

where q is the phonon wave vector, $\omega(q)$ is the phonon frequency in the dispersion curve, Γ is the natural line width and L_c is the localization length of the optical phonons. On the other hand, if the phonons propagate along a large single crystal, describing an infinite localization length, the corresponding Raman peak will present a perfect symmetric shape. In this context, the asymmetric characteristic of TO peak lead us to assert that the optical phonons are strongly localized in the nanowires. HRTEM images suggest that the origin of the phonon localization can be associated with polycrystallites in the shell since the variation of crystalline orientation in each crystallite could prevent the propagation of phonons. In order to determine the localization length of optical phonons the theoretical Raman spectrum in TO region was calculated using equation (1). The phonon dispersion curve $\omega(q)$ was taken from [31]. Figure 2(b) depicts the best fit (green line) to the experimental (diamonds) spectrum resulting in an average size of $L_c = 3$ nm, i.e. the same order of magnitude of the grains in the polycrystalline shell, as can be seen in TEM image of figure 2(c).

In our phonon localization analysis we have neglected any influence of the crystalline cores. From HRTEM images we notice that the diameter of the crystalline core is less than one-third of the total wire diameter. So, the ratio between the volume of the core and the volume of the amorphous/polycrystalline layer is estimated to be less than one to eight. Besides the diminutive scattering volume of the cores in comparison with the polycrystalline shells, we have also to consider the strong attenuation of the 514.5 nm laser in InP. The light intensity exponentially decreases during the propagation through the polycrystalline shells, resulting in a maximum penetration depth of 60 nm, which also contribute to the suppression of the Raman signal of inner crystalline portions.

At first sight, the calculation of the phonon localization length could also be performed by adopting a similar approach with LO peak. Since LO phonons in InP present a negative dispersion, the contribution of phonons with $q > 0$ to the Raman spectrum will result in a downward asymmetric line. In fact the LO peak in figure 2(a) presents the expected asymmetry. However, the LO line shape can also be affected by effects other than quantum confinement, such as coupling between LO phonons and plasmons that can be present in nanowires surfaces. In this case, the resulting line shape is determined by a competition of these two effects and the application of the localization model on LO peak would lead to an incorrect value for the localization length. On the other hand, TO phonons cannot couple with carrier excitations and the observed asymmetry of the line will only be a consequence of the phonon localization, enabling a more accurate evaluation for L_c.

3.2. Device fabrication and transport mechanisms

Substrates were found to be uniformly covered by a thick layer of nanowires (see figure 1) after the growth. Different devices were built, trying out a sort of metals for the electrodes, but only Ti and Ni exhibited ohmic behaviour, suited for temperature dependent resistance measurements, as shown

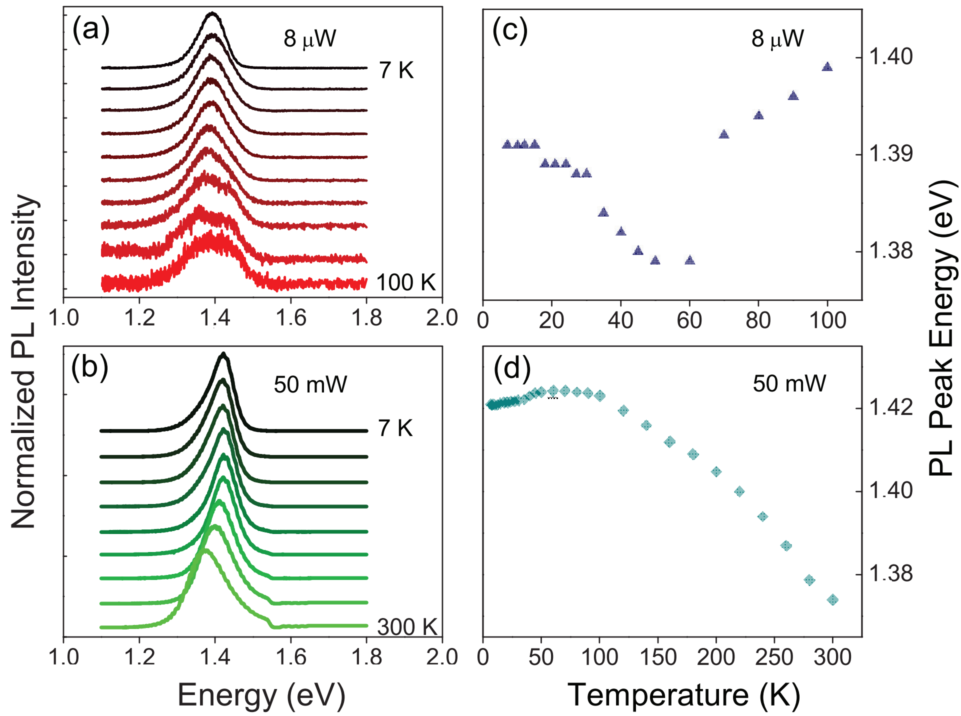

Figure 4. Photoluminescence spectra for different temperature values and for (a) 8 μW and (b) 50 mW power excitations. Panels (c) and (d) show the PL peak energy behaviour as a function of temperature for both laser intensities.

in figure 3(a). Also, by studying a dispersion of nanowires we obtain parameters which statistically represent the mean response of the system avoiding errors when choosing a particular nanowire.

The typical temperature dependent resistance of a semiconductor was observed for our devices as presented in figure 3(b), in which the resistance exponentially decreases as the temperature increases. The observed curve does not follow the simple thermal excitation law for a semiconductor [32], requiring a more detailed investigation to determine the dominant carrier transport process.

Even when nanowires exhibit a crystalline core, any considerable degree of disorder can lead to a localized behaviour of carriers, especially near surfaces [33]. It is believed that the amorphous/polycrystalline layer around the crystalline core (see HRTEM analysis) is the corresponding source of disorder, randomizing the electron potential at the core-shell interface and inducing localized states; otherwise, the shell itself is acting as a conduction channel. By taking into account these considerations, the usual thermally excited transport mechanism observed in semiconductor crystals should be replaced by a more complex one such as the variable range hopping (VRH) originally due to Mott and described by [34]

$$R(T) = R_0 \exp\left(\frac{T_0}{T}\right)^p, \tag{2}$$

where R_0 and T_0 are constants and the exponent p being set to 1/4, 1/3 or 1/2 according to the dimensionality of the samples [35, 36]. This model assumes that localized states around Fermi level trap carriers and the transport occurs by hops of charges from a localized state to another. According to Mott's model, the hopping range, R_{hopping} is given by [34]

$$R_{\text{hopping}}(T) = \left\{\left(\frac{7,6}{T_0 k_B N}\right)^{1/3}\left(\frac{3}{2\pi N k_B T}\right)\right\}^p, \tag{3}$$

where k_B is Boltzmann's constant and N is the density of states at the Fermi level. Fitting of equation (2) to experimental data leads to a p-value of 1/4 which corresponds to a 3D structure (p was one of the adjustable parameters during the fitting procedure). The good agreement between the experimental data and theoretical values for temperatures ranging from 100 K to 250 K is clearly seen in figure 3(c). Below 100 K, the samples' response is negligible and above 250 K the effect of thermal excitation begins to appear. The R_{hopping} values near room temperature (250 K) are plotted in figure 3(d) and are similar for all devices measured. These values were found around 10 nm and correspond to the distance that electrons must hop in order to contribute to the conductivity. This length is near ten times smaller than nanowire cross-sections, confirming that the nanostructures studied in this work do behave as 3D systems.

As a consequence of VRH processes, the localized states are pointed out as the main factor contributing to changes in electric resistance of the samples. The influence of localized states is so strong that temperatures even close to the room temperature, which are usually high for this mechanism, were not enough to affect the transport significantly.

3.3. Optical response

In order to further study the influence of the localized states on the optical response of the system, photoluminescence measurements were carried out as a function of temperature.

Figures 4(a) and (b) display a series of photoluminescence spectra over a large temperature range for low (8 μW) and high laser power density (50 mW), respectively. The PL spectra taken in low excitation power show Gaussian shapes at low temperatures, where the main peak positions are associated to the ground state of electron-heavy hole (e-hh) excitonic transitions. PL peak redshifts by $\sim$17 meV when the temperature increases from 10 to 50 K. By further increasing the temperature from 60 to 100 K, the PL peak energy blueshifts by $\sim$20 meV and a shoulder at the higher energy side of the spectrum can be observed. The relative intensity of the ground state peak increases as the temperature increases in this range, which can be assigned to the thermal excitation of carriers to the first excited state. Such behavior is not observed when a high laser power density is used, as shown in figure 4(b). In this case, the high band filling effect leads to an overall blueshift of the PL spectra at temperatures above 100 K. For further heating, the PL spectrum of the sample develops small asymmetry at the higher energy side and the PL peak position shows the usual temperature dependent band gap shrinkage.

Temperature dependence of the band gap and/or exciton energies in bulk and heterostructure semiconductors have been extensively studied in the last decades. It is also well known that the band gap energy normally shrinks when the temperature increases due to electron–phonon interaction and lattice thermal expansion. In order to describe the dependence of exciton transition/band gap energies on temperature, different models have been proposed, for example, the ones developed by Varshni, Vinã and Pässler [37–40]. Sometimes these models have limitations to describe the gap versus temperature behavior in semiconductor when different scattering mechanism in the material modulates the band structure and leads to unusual temperature dependent recombination process [41, 42], like the S and V-shape reported in many works, including bulk, quantum wells and quantum wires nanostructures [43–46]. At low excitation power and low temperature regimes, the photo-excited carriers are subject to the influence of potential fluctuation resulting from imperfections during of growth, like intermixing of material along the interfaces, defects, segregation an diffusion of atoms along the lattice [47, 48]. These fluctuations induce band tail in the excitonic density of state below the fundamental energy gap state and generated photo-carriers relax to lower energy states of the confinement potential when the sample is heated thus, leading to a decrease of the recombination peak energy.

When the temperature is further increased, the carriers may be thermally activated to higher energy levels, leading to a blueshift of the recombination spectrum by filling the whole states available. From this point of view, the regular reduction of the band gap energy is observed for larger values of temperature. Figures 4(c) and (d) shows the effects of temperature on the PL peak energy. By comparing the changes on the PL peak energy as function of temperature measured with two different laser power densities, one sees that the PL signal is weak at low power and, by heating the sample, the e-hh excitonic recombination channel becomes easily quenched. The V-shape observed in this regime clearly demonstrates a very strong influence of the potential fluctuations on the optical exciton recombination. As already reported in another papers [43, 44], the laser intensity increasing leads to a decreasing in the magnitude of the V-shape line. The regular dependence of gap and excitonic transition energies versus temperature can be recovered once the fluctuation profiles become screened in the regime of high photo-excited carriers. However, even using a high density laser power, as displayed in figure 4(d), traces of the presence of potential fluctuation in the low temperature regime can still be observed, which clearly demonstrates that the amorphous/polycrystalline shell of the nanowires dominates excitonic recombinations in any laser power regime.

4. Conclusions

InP nanowires with single crystalline zincblend core and polycrystalline/amorphous shell were synthesized from a reliable route without the use of hazardous precursors. The amorphous/polycrystalline shell showed a remarkable influence in the nanowires structural, electrical and optical properties. Structurally, polycrystallites in the shell produced phonon localization effects noticeable in the asymmetric shape of TO peaks of Raman spectra performed in as-grown samples. Analysis of these spectra allowed to determine the phonon localization length which presented the same order of magnitude of the polycrystallite sizes, indicating that the variation of crystalline orientation in each crystallite prevents the propagation of phonons. Concerning the electrical properties, samples behaved as a semiconductor material. However, the better fitting for the dominant transport mechanism was not the commonly expected simple thermal activation but the variable range hopping mechanism. This result was explained by the interplay between disorder and localization which randomizes the electron potential at the core-shell interface thus, inducing localized states and leading to the hopping mechanism. Indeed, the presence of disorder should affect all the properties of the samples. Additional optical investigations were conducted and confirmed that disorder plays an important role in samples properties. By observing the PL peak energy as function of temperature it was found S and V-shaped curves, even using high density laser power, indicating that the potential fluctuations are strong enough to affect the excitonic recombination in these conditions. These results agree and confirm the presence of disorder and, consequently, the fluctuations in electronic potential observed in transport measurements. In fact, this is also an additional evidence of a transition from thermally activated electronic excitation to a more complex process such as the variable range Mott-like hopping.

Acknowledgments

The authors thank the financial support from the Brazilian agencies: grants 2012/06916-4, 2013/18719-1 and 2014/07375-2, São Paulo Research Foundation (FAPESP) and grants 302640/2010-0 and 471191/2013-2, CNPq. We also thank Dr C J Dalmaschio for TEM images.

References

[1] Hobbs R G, Petkov N and Holmes J D 2012 *Chem. Mater.* **24** 1975
[2] Strupeit T, Klinke C, Kornowski A and Weller H 2009 *ACS Nano* **3** 668
[3] Wallentin J *et al* 2013 *Science* **339** 1057
[4] Weinberg I and Drinker D J 1986 *Indium Phosphide Solar Cells—Status and Prospects for Use in Space, 21st Intersociety Energy Conversion Engineering Conf. (San Diego, 25–29 August 1986)*
[5] Yoshimura M, Nakai E, Tomioka K and Fukui T 2013 *Appl. Phys. Express* **6** 052301
[6] Wang J, Gudiksen M S, Duan X, Cui Y and Lieber C M 2001 *Science* **293** 1455
[7] Wang Z *et al* 2013 *Nano Lett.* **13** 5063
[8] Maeda S, Tomioka K, Hara S and Motohisa J 2012 *Japan J. Appl. Phys.* **51** 02BN03
[9] Li K, Sun H, Ren F, Ng K W, Tran T D, Chen R and Chang-Hasnain C J 2014 *Nano Lett.* **14** 183
[10] Cui Y *et al* 2013 *Nano Lett.* **13** 4113
[11] Liu C, Dai L, You L P, Xu W J and Qin G G 2008 *Nanotechnology* **19** 465203
[12] Hui A T, Wang F, Han N, Yip S, Xiu F, Hou J J, Yen Y, Hung T, Chueh Y and Ho J C 2012 *J. Mater. Chem.* **22** 10704
[13] Lopez-Richard V, González J C, Matinaga F M, Trallero-Giner C, Ribeiro E, Dias M R S, Villegas-Lelovsky L and Marques G E 2009 *Nano Lett.* **9** 3219
[14] Dias M R S, Lopez-Richard V, Ulloa S E, Castelano L K, Rino J P and Marques G E 2012 *Appl. Phys. Lett.* **101** 182104
[15] Tsuzuki H, Cesar D F, Dias M R S, Castelano L K, Lopez-Richard V, Rino J P and Marques G E 2011 *ACS Nano* **5** 5519
[16] Kunets V P, Teodoro M D, Dorogan V G, Lytvyn P M, Tarasov G G, Sleezer R, Ware M E, Mazur Yu I, Krasinski J S and Salamo G J 2010 *Appl. Phys. Lett.* **97** 262103
[17] Kunets V P, Prosandeev S, Mazur Yu I, Ware M E, Teodoro M D, Dorogan V G, Lytvyn P M and Salamo G J 2011 *J. Appl. Phys.* **110** 083714
[18] Zhang L, Luo J, Zunger A, Akopian N, Zwiller A and Harmand J 2010 *Nano Lett.* **10** 4055
[19] Faria P E Jr, Campos T and Sipahi G M 2014 *J. Appl. Phys.* **116** 19350
[20] Greta R, Patzke G R, Kontic R, Shiolashvili Z, Makhatadze N and Jishiashvili D 2013 *Materials* **6** 85
[21] Gudiksen M S, Wang J and Lieber C M 2001 *J. Phys. Chem.* B **105** 4062
[22] Haapamaki C M and LaPierre R R 2011 *Nanotechnology* **22** 335602
[23] Algra R E, Verheijen M A, Borgström M T, Feiner L F, Immink G, van Enckevort W J P, Vlieg E and Bakkers E P A M 2008 *Nature* **456** 369
[24] Berengue O M, Simon R A, Leite E R and Chiquito A J 2011 *J. Phys. D: Appl. Phys.* **44** 215405
[25] Pusep Yu A, Chiquito A J, Mergulhão S and Galzerani J C 1997 *Phys. Rev.* B **56** 3892
[26] Pusep Yu A, Chiquito A J, Mergulhão S and Toropov A I 2002 *J. Appl. Phys.* **92** 3830
[27] Wagner R S and Ellis W C 1964 *Appl. Phys. Lett.* **4** 89
[28] Kamimura H, Dalmaschio C J, Carrocine S C, Rodrigues A D, Gouveia R C, Leite E R and Chiquito A J 2015 *J. Mater. Res. Express* **2** 045012
[29] Seong M J, Mićić O I, Nozik A J and Mascarenhas A 2003 *Appl. Phys. Lett.* **82** 13
[30] Campbell I H and Fauchet P M 1986 *Solid State Commun.* **58** 739
[31] Borcherds P H, Alfrey G F, Woods A D B and Saunderson D H 1975 *J. Phys. C: Solid State Phys.* **8** 2022
[32] Yu P and Cardona M 2010 *Fundamentals of Semiconductors* (Berlin: Springer)
[33] Simon R A, Kamimura H, Berengue O M, Leite E R and Chiquito A J 2013 *J. Appl. Phys.* **114** 24370
[34] Mott N F and Davis E A 2012 *Electronic Processes in Non-crystalline Materials* (Oxford: Clarendon)
[35] Kamimura H, Araujo L S, Berengue O M, Amorim C A and Chiquito A J 2012 *Physica* E **44** 1776
[36] Han H S, Davis C and Nino J C 2014 *J. Phys. Chem.* C **118** 9137
[37] Varshni Y 1967 *Physica* **34** 149
[38] Vinã L, Logothetidis S and Cardona M 1984 *Phys. Rev.* B **30** 1979
[39] Pässler R 1998 *J. Appl. Phys.* **83** 3356
[40] Pässler R 1997 *Phys. Status Solidi* b **200** 155
[41] Lee C Y, Wu M C, Shiao H P and Ho J W 2000 *J. Cryst. Growth* **208** 137
[42] Pässler R 2002 *Phys. Rev.* B **66** 085201
[43] Duarte J L, Poças L C, Laureto E, Dias I F L, Lopes E M and Lourenço S A 2008 *Phys. Rev.* B **77** 165322
[44] Teodoro M D, Dias I F L, Laureto E, Duarte J L, González-Borrero P P, Lourenço S A, Mazzaro I, Marega E Jr and Salamo G J 2008 *J. Appl. Phys.* **103** 093508
[45] Dixit V K, Porwal S, Singh S D, Sharma T K, Ghosh S and Oak S M 2014 *J. Phys. D: Appl. Phys.* **47** 065103
[46] Bell A, Srinivasan S, Plumlee C, Omiya H, Ponce F A, Christen J, Tanaka S, Fujioka A and Nakagawa Y 2004 *J. Appl. Phys.* **95** 4670
[47] Elissev P G, Perlin G, Lee J and Osiński M 1997 *Appl. Phys. Lett.* **71** 569
[48] Elissev P G 2003 *J. Appl. Phys.* **93** 5404